Journal of Power Sources 248 (2014) 1191–1196

Contents lists available at ScienceDirect

Journal of Power Sources

journal homepage: www.elsevier.com/locate/jpowsour

# Effect of polymeric binder type on the thermal stability and tolerance to roll-pressing of spherical natural graphite anodes for Li-ion batteries

Yoon-Soo Park [a], Eun-Suok Oh [b,**], Sung-Man Lee [a,*]

[a] Department of Nano Applied Engineering, Kangwon National University, Chuncheon, Kangwon-Do 200-701, Republic of Korea
[b] School of Chemical Engineering, University of Ulsan, 93 Daehak-ro, Ulsan 680-749, Republic of Korea

## HIGHLIGHTS

- Spherical natural graphite anodes are prepared using PAA, CMC/SBR and PVDF binder.
- The effect of polymeric binder on the thermal stability is investigated.
- Tolerance to roll-press of S-NG anodes with different binders is investigated.
- The PAA binder effectively suppresses heat evolution at low temperatures.
- The PAA electrode maintains appropriate porous structure even at high electrode density.

## ARTICLE INFO

*Article history:*
Received 21 August 2013
Received in revised form
16 October 2013
Accepted 17 October 2013
Available online 25 October 2013

*Keywords:*
Spherical natural graphite
Anode
Binder
Polyacrylic acid
Thermal stability

## ABSTRACT

The polymeric binder is seen to affect the thermal stability and deformation of spherical graphite used in lithium ion battery anodes. Spherical natural graphite anodes are prepared using three different binders: two aqueous-based binders, polyacrylic acid (PAA) and a mixture of carboxy-methyl cellulose and styrene butadiene rubber (abbreviated CMC/SBR), and an organic-based binder, polyvinylidene fluoride (PVDF). The thermal stability of fully lithiated electrodes is measured by differential scanning calorimetry (DSC). The PAA binder effectively suppresses heat evolution (43% (PVDF) and 23% (CMC/SBR) less heat) at low temperatures up to 200 °C during DSC scans of the lithiated electrodes, compared to the PVDF and CMC/SBR binders. In addition, the PAA binder allows the graphite electrode to maintain an appropriate porous structure (13% greater porosity than the PVDF and CMC/SBR electrodes) even at high electrode density after 6 kgf $cm^{-2}$ compression, thus leading to enhanced effective cycles (11% (PVDF) and 60% (CMC/SBR) greater capacity after 50 cycles).



## 1. Introduction

In recent years, applications of Li-ion batteries (LIBs) have expanded to automotive power supplies and energy storage systems for intermittent renewable energy. Compared to mobile devices, these applications require a more stringent property profile that includes a strong safety profile, low cost, an environmentally friendly manufacturing process, high energy and power densities, and long cycle life, all of which are closely related to the electrode components. In composite electrodes of LIBs, the polymeric binder is an important component of the electrode formulation. The binder maintains the physical structure of the electrode by holding together active materials containing conductive additives with the current collector. A proper electrode formulation is critical to the development of high-performance batteries and thus the binder system should be optimized for a given electrode material to address the aforementioned issues.

Polyvinylidene fluoride (PVDF) has been widely used as a binder for typical LIBs because of its good electrochemical stability and adhesion to both active materials and the current collector. Its disadvantages include, however, high cost, the use of organic solvents, e.g., N-methyl-2-pyrrolidone (NMP), and the requirement of tight humidity control during processing [1,2]. Additionally, the disposal of PVDF at the end of the battery life is not straightforward [3]. On the other hand, water-soluble binders such as carboxymethyl cellulose (CMC) and styrene butadiene (SBR) use water as

* Corresponding author. Tel.: +82 33 250 6266; fax: +82 33 250 6260.
** Corresponding author. Tel.: +82 52 259 2783; fax: +82 52 259 1689.
*E-mail addresses:* esoh1@ulsan.ac.kr (E.-S. Oh), smlee@kangwon.ac.kr (S.-M. Lee).

0378-7753/$ – see front matter © 2013 Elsevier B.V. All rights reserved.
http://dx.doi.org/10.1016/j.jpowsour.2013.10.076

the processing solvent, leading to an environmentally friendly LIB manufacturing process that can be performed at a lower cost since solvent recycling is not necessary. Due to these advantages, water-soluble binders have gradually replaced conventional PVDF binders in the preparation of LIB anodes composed of graphite [2,4–9] and high-capacity materials containing Si or Sn [7,10–14].

Natural graphite is the most commonly used anode material in current LIBs due to its high reversible capacity and low cost. Spherical natural graphite is especially preferred because the spherical geometry is favorable to the diffusion of $Li^+$ ions from the electrolyte surrounding the graphite active materials. Unfortunately, spherical natural graphite, formed by the folding of small graphite flakes, is easily deformed during electrode compression. Therefore, both electrode loading and porosity control by compression greatly influence the electrochemical performance of spherical natural graphite anodes. Electrode compression is one of the key factors in finding an appropriate polymeric binder to optimize electrode loading and porosity.

With respect to safety issues, it is necessary to investigate the effect of polymeric binders on the thermal stability of carbon anodes, especially heat evolution at low temperatures below 200 °C, which may lead to uncontrollable thermal runaway in LIBs [15–18]. Few studies, however, have been conducted on the thermal stability of spherical natural graphite electrodes containing water-soluble binders.

In this work, the effect of polymeric binder type on the thermal stability and electrochemical performance of spherical natural graphite anodes is investigated. Polyacrylic acid (PAA) and a mixture of CMC and SBR (abbreviated CMC/SBR) are chosen as water-soluble binders, and results with these binders are compared to those obtained with PVDF binder.

## 2. Experimental

Spherical natural graphite electrodes coated with PVDF (KF1100, Kureha, Japan), PAA (Noverite™ K-702 Polymer, Lubrizol, USA), or CMC (2200, DAICELL, Japan)/SBR (BM-480B, ZEON, Japan) (1:1) were prepared as follows. Spherical natural graphite (POSCO Chemtech Co. Ltd. SNG10) powder (95 wt.%) was mixed with the binder (5 wt.%) in a dispersion medium (NMP for PVDF, distilled water for PAA and CMC/SBR) to obtain a slurry. The slurry was spread on copper foil and was dried under vacuum for 12 h at 120 °C (for PVDF) or 180 °C (for PAA and CMC/SBR). Normally, conventional anodes contain typical conductive materials such as super-P to enhance the electrical conducting behavior. Some irreversible capacity during initial cycling, however, is caused by conductive materials, which can affect differential scanning calorimetry (DSC) results. In this work, conductive material additives were not used in order to be able to observe the intrinsic behavior of graphite anodes with different binders. After drying, the electrodes were compressed using a roll press at 2, 3, 4, and 6 kgf $cm^{-2}$. Surface images of the electrodes were obtained using a scanning electron microscope (SEM).

For electrochemical measurements, CR2016-type coin cells with a working electrode and a lithium foil counter electrode were assembled in an Ar-filled glovebox. The electrolyte was 1 M $LiPF_6$ in a mixture of ethylene carbonate and diethyl carbonate (1:1 by volume, provided by PANAX ETEC Co. Ltd, Korea). The cells were charged (intercalated) and discharged (deintercalated) between 0.005 and 2.0 V at 30 °C. The cells were charged in constant current-constant voltage mode, consisting of constant current at 70 mA $g^{-1}$ followed by constant voltage at 0.005 V until the current decreased to 7 mA $g^{-1}$, and were discharged at a constant current of 70 mA $g^{-1}$.

For DSC measurements, cells were galvanostatically pre-cycled three times to reach a stable capacity level, and the cycling was interrupted when the cells were charged to a fully intercalated state. The charged cells were disassembled in a glovebox. Discs of 0.5 cm diameter with a Cu current collector were cut from the electrode sheet without removing the electrolyte and were transferred to a high-pressure stainless steel pan with a gold-plated copper seal. DSC scans were performed using a DSC 200 F3 (NETZSCH, Germany) at a heating rate of 5 °C $min^{-1}$.

Powder X-ray diffraction (XRD) with Cu $K_\alpha$ radiation was used to identify the lithiated state and structural characteristics of graphite electrodes as a function of temperature. The samples for XRD analysis were prepared by heating fully lithiated samples to the designated temperature in the DSC, followed by rapid cooling to room temperature.

## 3. Results and discussion

The thermal stability of Li-ion batteries is correlated with the thermal reaction and/or decomposition of cell components, particularly in fully charged cells. Fig. 1 showed the thermal behavior of graphite electrodes with different binders, measured by DSC, where DSC profiles were determined by subtracting the baseline, obtained by subsequent heating, from the initial profile. Before DSC measurements, the graphite electrodes were pre-cycled three times and then charged to the fully intercalated state. The broad exothermic reaction observed below 200 °C is significantly reduced when PAA is used as the binder. The exothermic process at temperatures below 140 °C is mainly ascribed to thermal decomposition of the solid electrolyte interface (SEI) film formed during initial cycling, and subsequent heat evolution is due to the reaction between the intercalated lithium and the electrolyte after SEI layer breakdown [19–23]. As shown in Fig. 2, the initial reversible capacity/Coulombic efficiency of electrodes with PVDF, CMC/SBR and PAA binders were 348/88.5, 351/90.3 and 349/90.1 mAh $g^{-1}$/%, respectively. Thus, electrodes with PVDF, CMC/SBR and PAA binders exhibited initial irreversible capacities of 45, 37 and 35 mAh $g^{-1}$, respectively. It is noticed that the amount of heat generated below 140 °C in Fig. 1(b) is in the same order as the initial irreversible capacity, i.e. the PVDF-containing electrode generates more heat than the other binder-containing electrodes, whereas the CMC/SBR- and PAA-containing electrodes show similar heat generation. Above 140 °C, however, the PAA binder electrode generates a smaller amount of heat than the CMC/SBR binder electrode as shown in Fig. 1(b).

The overall heat generation of electrodes calculated from the DSC curves of Fig. 1(a) as a function of temperature is shown in Fig. 3. The PAA electrode generates the smallest amount of heat at temperatures up to 400 °C, while the onset temperatures of the exothermic reaction for the three samples are very similar. Since heat generation after SEI layer decomposition results from deintercalation of lithium in the graphite at elevated temperatures [19–23], the results shown in Fig. 3 indicate that the delithiation process at elevated temperatures is considerably suppressed when PAA is used as a binder. This result is supported by XRD analysis (Fig. 4) of the lithiated electrodes with different binders, which are heated to the temperature designated in the DSC curve of Fig. 1 followed by rapid cooling to room temperature.

When the electrode samples are heated to 230 °C, the Bragg peak corresponding to Stage-1 structure is still evident in the diffraction pattern of the PAA electrode, while this peak almost completely disappears in the diffraction patterns of the PVDF and CMC/SBR electrodes. This finding indicates that more lithium is extracted from the latter electrodes, especially the PVDF electrode, compared to the PAA electrode. The exceptionally low delithiation in the PAA electrode can be explained as follows. Magasinski et al. [24] reported that numerous carboxyl groups in the PAA binder

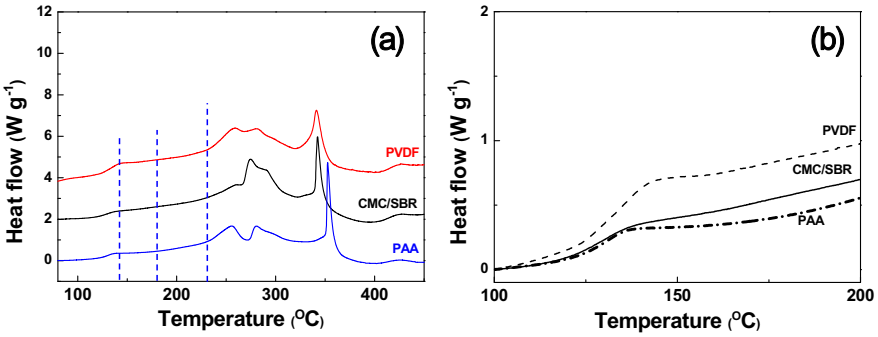


**Fig. 1.** DSC curves of spherical natural graphite electrodes with different binders in the fully lithiated state with electrolyte (a) at temperatures up to 450 °C, and (b) at temperatures to 200 °C.

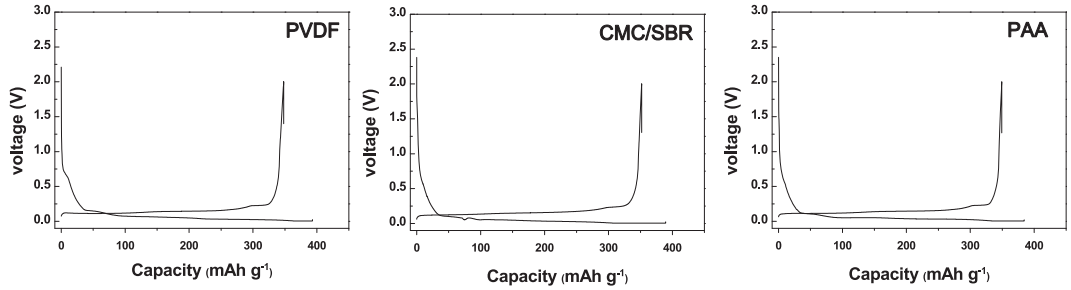


**Fig. 2.** The charge–discharge curves of spherical natural graphite electrodes fabricated with different binders in 1 M $LiPF_6$ in EC-DEC (1:1, v/v) electrolyte.

formed strong hydrogen bonds with the carbon-coated silicon nanopowders that contain functional groups on their surface. Using X-ray photoelectron spectroscopy, Park et al. [25] showed that strong hydrogen bonds contributed to the homogeneous distribution of binder on the active material surface. Thus, the graphite particles are uniformly covered with a thin layer of PAA due to the strong interaction between the particles and the PAA binder, whereas the PVDF binder, which forms weak hydrogen bonds with active materials, does not cover the entire surface of graphite particles [25] allowing swelling with the intake of electrolyte to occur [6–8,26]. The thin PAA layer acts as a protective film that inhibits direct contact between graphite and the electrolyte. Consequently, the PAA binder layer strongly suppresses the delithiation process at elevated temperatures since the diffusivity of lithium ions in the polymer layer is significantly lower than in the solid electrolyte interface [27]. In addition, greater surface coverage leads to lower initial irreversible capacity and heat generation in the PAA-containing electrode by suppressing the formation of the SEI compared to the PVdF- and CMC/SBR-containing electrodes.

Performance of spherical natural graphite anodes is greatly influenced by electrode loading and porosity, because spherical natural graphite is easily deformed during electrode compression. Fig. 5 shows surface images of electrodes with different binders as a function of applied pressure, which is ranged from 2 to 6 kgf $cm^{-2}$ during electrode fabrication. Upon increasing pressure on the electrode, spherical natural graphite particles are pressed flat, particular at the outer surface, yielding a decrease in electrode porosity. The reduction of electrode surface porosity is most noticeable for the electrode with PVDF binder, followed by the electrodes with CMC/SBR and PAA binders. The electrode containing PAA appears to be the most resistant to pressing and maintains a porous structure even with a high roll press pressure. Accordingly, the densities of the PVdF- and CMC/SBR-containing electrodes increase sharply with preparation pressure whereas the PAA-containing electrode shows a gradual increase in density according to the pressure, as displayed in Fig. 6. The densities of the obtained electrodes appear to be higher than 1.5 g $cm^{-3}$, a value that is typical for real applications of spherical natural graphite electrodes. These results are closely related to the mechanical properties of the binder. Concerning tensile strength, PAA has the highest stress at break of about 90 MPa [28], compared to CMC and PVDF whose stresses at break are 30 MPa [29] and 37 MPa [30], respectively. The elongation of PVDF is above 50% [31], whereas CMC and PAA possess low percentages of elongation [9,29]. The addition of the elastomeric additive SBR to CMC yields an increased elongation and a lower tensile strength for CMC/SBR compared to CMC alone [31].

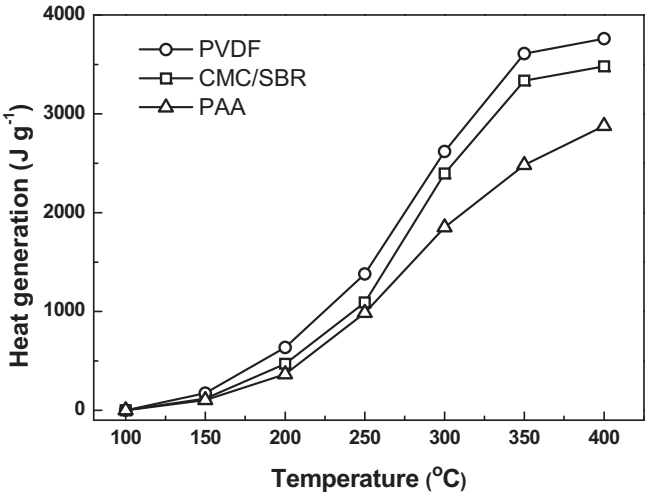


**Fig. 3.** Overall heat evolution from spherical natural graphite electrodes fabricated with different binders in the fully-lithiated state as a function of temperature.

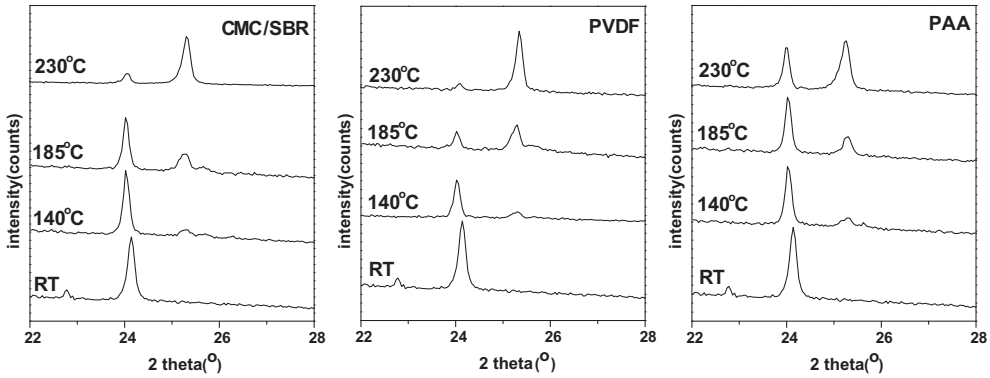


**Fig. 4.** XRD patterns of spherical natural graphite electrodes heated to a designated temperature in DSC (Fig. 1) as a function of binder type.

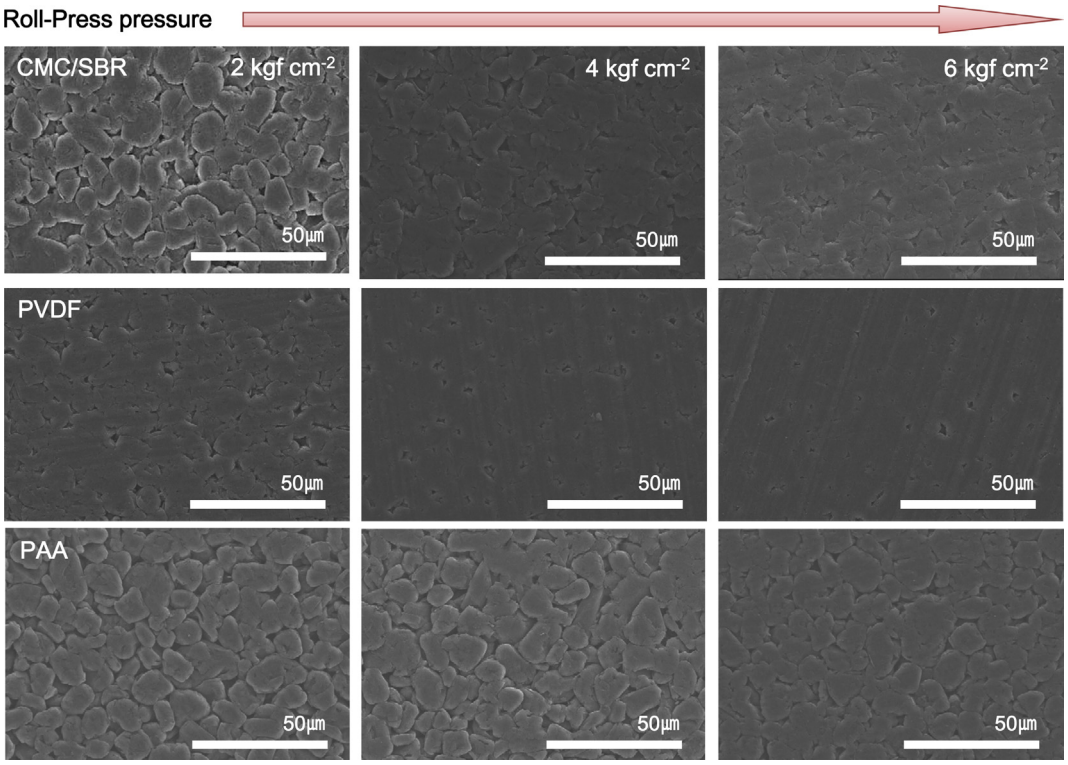


**Fig. 5.** SEM images of electrode surfaces showing the effects of different binders as a function of applied pressure during electrode fabrication.

The reduction of electrode porosity by pressing increases its conductivity but decreases its capacity due to transport limitations within the liquid path [32,33]. Therefore, the ability of PAA to effectively modify the surface and to aid in maintaining the electrode porous structure through its rigidity leads to superior electrochemical performance of electrodes formulated with PAA. This result is seen in Fig. 7, which displays the cyclic performance of electrodes as a function of preparation pressure.

The PAA-containing electrodes exhibit excellent cycling stability regardless of the fabrication pressure, while the capacity fading of the other electrodes containing either PVDF or CMC/SBR binder becomes more pronounced as the preparation pressure is increased. Interestingly, the PVDF electrode is less affected by preparation pressure than the CMC/SBR electrode, although the PVDF electrode becomes denser at high roll-press pressure compared to the CMC/SBR electrode as shown in Figs. 5 and 6. This result is due to the fact that PVDF is more easily swollen by electrolyte solution than CMC and PAA [26]. As shown in Fig. 8, the

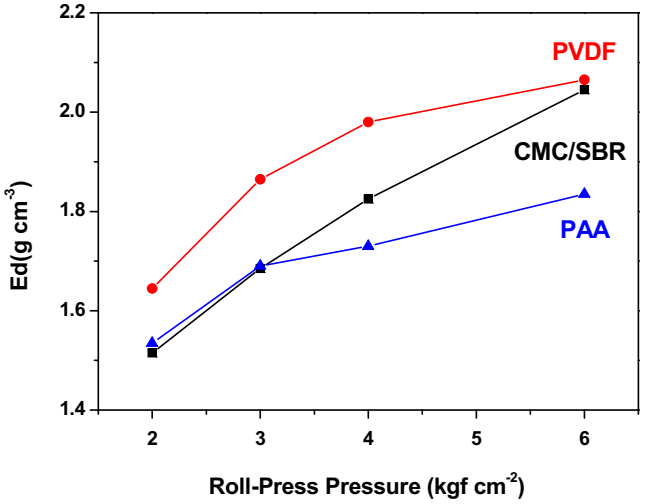


**Fig. 6.** Densities of spherical natural graphite electrodes fabricated with different binders as a function of applied pressure during electrode fabrication.

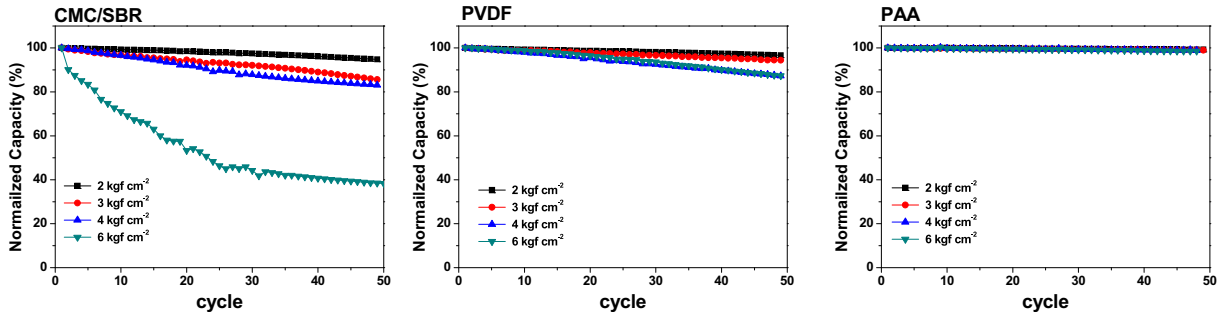


**Fig. 7.** Cycle performance of spherical natural graphite electrodes fabricated with different binders as a function of applied pressure during electrode fabrication.

thickness of the PVDF electrode pressed at 6 kgf $cm^{-2}$ increases after soaking in electrolyte for 12 h, whereas no apparent change in the thickness of CMC/SBR and PAA electrodes is observed. The swollen PVDF electrode exhibits high ionic conductivity due to the absorbed electrolyte, which gives rise to better electrochemical stability at high roll-press pressure compared to the CMC/SBR electrode. The electrolyte absorption by the binder, however, can weaken its adhesion strength. In the case of the PAA-containing electrode, the rigidity of the PAA binder maintains the porosity of the electrode even at high preparation pressure and prevents excess electrolyte absorption, leading to facile electrolyte swelling of the electrode without loss of adhesion. The surface morphologies of 50-cycled graphite electrodes with different binders prepared by compression at 6 kgf $cm^{-2}$ were characterized by SEM (Fig. 9). The corresponding fresh electrodes before cycle testing were in Fig. 5. The SEM images reveal that the PAA containing electrode maintains its porous structure even after 50 cycles. This result is mainly due to numerous carboxyl groups in the PAA binder forming strong hydrogen bonds with natural graphite leading to a homogeneous distribution of binder on the surface of active materials, which suppresses formation of the SEI layer during cycling compared to electrodes prepared with PVDF and CMC/SBR binders. The surface

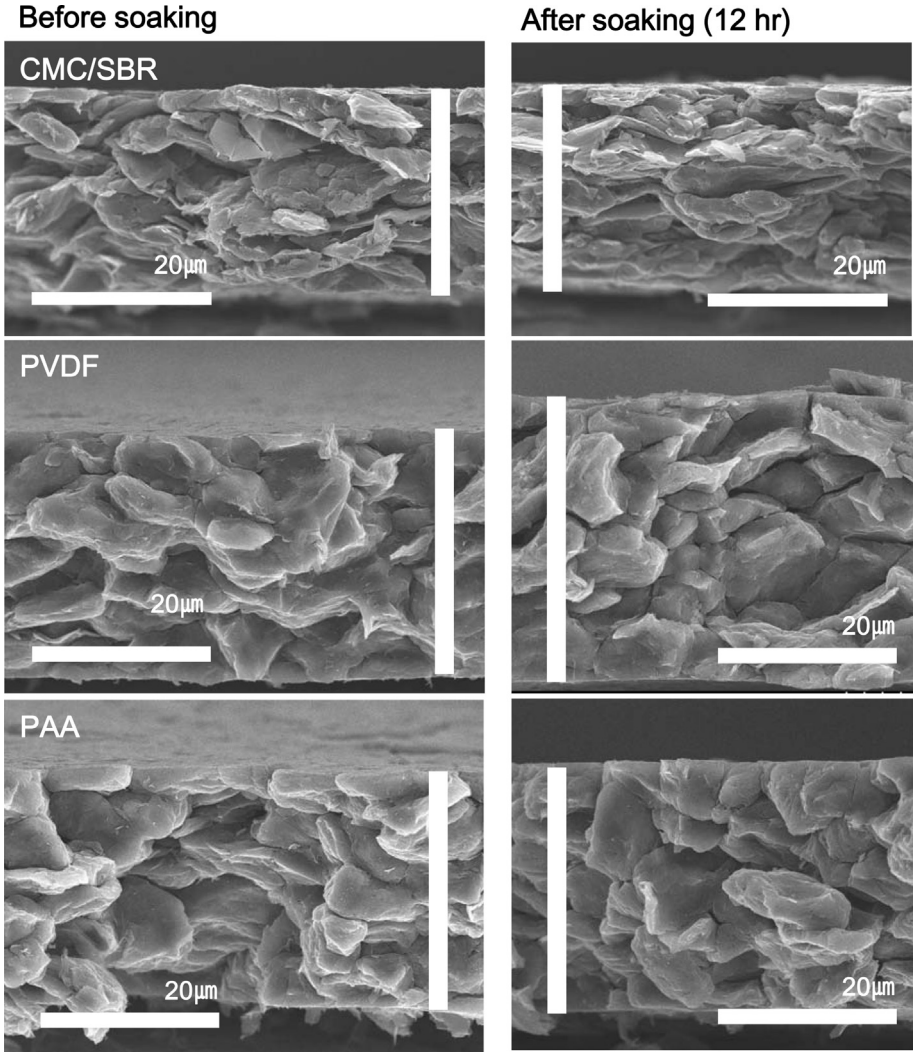


**Fig. 8.** Cross-sectional SEM images of spherical natural graphite electrodes, pressed at 6 kgf $cm^{-2}$, after soaking in electrolyte solution for 12 h.

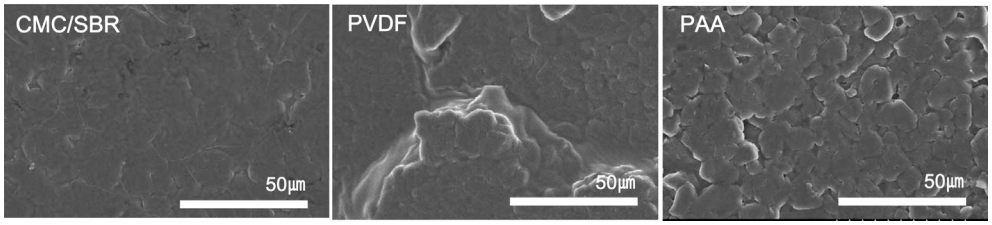


**Fig. 9.** SEM images of electrode surface morphologies of graphite electrodes fabricated with different binders, pressed at 6 kgf $cm^{-2}$, after 50 cycles.

of the CMC/SBR electrode is covered with a thick SEI film after cycling, and a porous structure is difficult to find. On the other hand, for the PVDF electrode, a bumpy morphology with some cracks is observed on the outer surface as a result of swelling by electrolyte solution, although it has a less porous surface structure before soaking in electrolyte and cycling.

Consequently, these results demonstrate that PAA is a superior binder for the formulation of spherical natural graphite anodes.

## 4. Conclusions

Spherical natural graphite anodes prepared using the aqueous-based binders PAA and CMC/SBR, and an organic-based binder, PVDF, are evaluated for their thermal stability in the fully lithiated state. Additionally, the surface morphology and cycle performance of the electrodes are also investigated as a function of electrode density. Surface coverage in the PAA-containing electrode gives rise to a reduction of thermal evolution caused by the delithiation during DSC scanning compared to electrodes prepared with PVDF and CMC/SBR binders. This factor also contributes to the lower initial irreversible capacity of the electrode containing PAA binder. The PAA electrodes are the most resistant to pressing and thereby are able to maintain a porous structure even at high electrode density, leading to enhanced cycle performance. PAA is therefore a promising candidate for a water-soluble, low-cost alternative to non-aqueous PVDF binder for spherical natural graphite anodes in Li-ion batteries.

## Acknowledgments

This study was supported by the National Research Foundation of Korea Grant funded by the Korean government (MEST) (NRF-2009-C1AAA001-0093307) and an Energy Efficiency & Resources from the Korea Institute of Energy Technology Evaluation and Planning (KETEP) funded by the Korea Government's Ministry of Knowledge Economy (project no. 2011201010016B).

## References

[1] A. Guerfi, M. Kaneko, M. Petitclerc, M. Mori, K. Zaghib, J. Power Sources 163 (2007) 1047–1052.
[2] F.M. Courtel, S. Niketic, D. Duguay, Y.A. -Lebdeh, I.J. Davidson, J. Power Sources 196 (2011) 2128–2134.
[3] S.F. Lux, F. Schappacher, A. Balducci, S. Passerini, M. Winter, J. Electrochem. Soc. 157 (2010) A320–A325.
[4] J. Drofenik, M. Gaberscek, R. Dominko, F.W. Poulsen, M. Mogensen, S. Pejovnik, J. Jamnok, Electrochim. Acta 48 (2003) 883–889.
[5] S.S. Zhang, K. Xu, T.R. Jow, J. Power Sources 138 (2004) 226–231.
[6] K. Ui, S. Kikuchi, F. Mikami, Y. Kadoma, N. Kumagai, J. Power Sources 173 (2007) 518–521.
[7] N.S. Hochgatterer, M.R. Schweiger, S. Koller, P.R. Raimann, T. Wohrle, C. Wurm, M. Winter, Electrochem. Solid-State Lett. 11 (5) (2008) A76–A80.
[8] S. Komaba, T. Ozeki, K. Okushi, J. Power Sources 189 (2009) 197–203.
[9] J. Chong, S. Xun, H. Zheng, X. Song, G. Liu, P. Ridgway, J.Q. Wang, V.S. Battaglia, J. Power Sources 196 (2011) 7707–7714.
[10] H. Buqa, M. Holzapfel, F. Krumeich, C. Veit, P. Novak, J. Power Sources 161 (2006) 617–622.
[11] B. Lestriez, S. Bahri, I. Sandu, L. Roue, D. Guyomard, Electrochem. Commun. 9 (2007) 2801–2806.
[12] S. Chibowski, E. Grzadka, J. Patkowski, Colloids Surf. 326 (2008) 191–203.
[13] D. Mazouzi, B. Lestriez, L. Roué, D. Guyomard, Electrochem. Solid-State Lett. 12 (11) (2009) A215–A218.
[14] J. Li, D.-B. Le, P.P. Ferguson, J.R. Dahn, Electrochimica Acta 55 (2010) 2991–2995.
[15] H. Maleki, G. Deng, A. Anani, J. Howard, J. Electrochem. Soc. 146 (1999) 3224–3229.
[16] D. Aurbach, J. Power Sources 89 (2000) 206–218.
[17] K. Edstrom, A.M. Andersson, A. Bishop, L. Fransson, J. Lindgren, A. Hussenius, J. Power Sources 97–98 (2001) 87–91.
[18] M. Yoshio, H.Y. Wang, K. Fukuda, Y. Hara, Y. Adachi, J. Electrochem. Soc. 147 (2000) 1245–1250.
[19] H.H. Lee, C.C. Wan, Y.Y. Wang, J. Electrochem. Soc. 151 (2004) A542–A547.
[20] H. Yang, H. Bang, K. Amine, J. Prakash, J. Electrochem. Soc. 152 (2005) A73–A79.
[21] Q. Wang, J. Sun, X. Yao, C. Chen, J. Electrochem. Soc. 153 (2006) A329–A333.
[22] M.N. Richard, J.R. Dahn, J. Electrochem. Soc. 146 (1999) 2068–2077.
[23] Y.S. Park, S.M. Lee, Electrochim. Acta 54 (2009) 3339–3343.
[24] A. Magasinski, B. Zdyrko, I. Kovalenko, B. Hertzberg, R. Burtovyy, C.F. Huebner, T.F. Fuller, I. Luzinov, G. Yushin, Appl. Mater. Interfaces 2 (2010) 3004–3010.
[25] H.K. Park, B.S. Kong, E.S. Oh, Electrochem. Commun. 13 (2011) 1051–1053.
[26] S. Komaba, K. Shimomura, N. Yabuuchi, T. Ozeki, H. Yui, K. Konno, J. Phys. Chem. C 115 (2011) 13487–13495.
[27] I. Kovalenko, B. Zdyrko, A. Magasinski, B. Hertzberg, Z. Milicev, R. Burtovyy, I. Luzinov, G. Yushin, Science 334 (2011) 75–79.
[28] X.D. Fan, Y.L. Hsieh, J.M. Krochta, M.J. Kurth, J. Appl. Polym. Sci. 82 (2001) 1921–1927.
[29] N.M. Antonova, Russ. J. Non-Ferrous Met. 50 (2009) 419–423.
[30] Z.H. Liu, P. Marechal, R. Jerome, Polymer 39 (1998) 1779–1785.
[31] W.R. Liu, M.H. Yang, H.C. Wu, S.M. Chiao, N.L. Wu, Electrochem. Solid-State Lett. 8 (2005) A100–A103.
[32] P. Novak, W. Scheifele, M. Winter, O. Haas, J. Power Sources 68 (1997) 267–270.
[33] J.S. Gnanaraj, Y.S. Cohen, M.D. Levi, D. Aurbach, J. Electroanal. Chem. 516 (2001) 89–102.